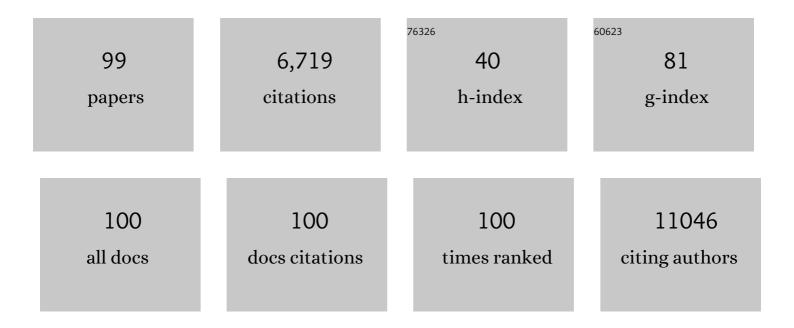
List of Publications by Year in descending order

Source: https://exaly.com/author-pdf/3026017/publications.pdf Version: 2024-02-01



MINA YOON

#	Article	IF	CITATIONS
1	Highly Responsive Ultrathin GaS Nanosheet Photodetectors on Rigid and Flexible Substrates. Nano Letters, 2013, 13, 1649-1654.	9.1	683
2	CO Oxidation on Supported Single Pt Atoms: Experimental and ab Initio Density Functional Studies of CO Interaction with Pt Atom on I-Al ₂ O ₃ (010) Surface. Journal of the American Chemical Society, 2013, 135, 12634-12645.	13.7	535
3	Calcium as the Superior Coating Metal in Functionalization of Carbon Fullerenes for High-Capacity Hydrogen Storage. Physical Review Letters, 2008, 100, 206806.	7.8	391
4	Interlayer Coupling in Twisted WSe ₂ /WS ₂ Bilayer Heterostructures Revealed by Optical Spectroscopy. ACS Nano, 2016, 10, 6612-6622.	14.6	249
5	Controlled Vapor Phase Growth of Single Crystalline, Two-Dimensional GaSe Crystals with High Photoresponse. Scientific Reports, 2014, 4, 5497.	3.3	222
6	Charged Fullerenes as High-Capacity Hydrogen Storage Media. Nano Letters, 2007, 7, 2578-2583.	9.1	220
7	Patterned arrays of lateral heterojunctions within monolayer two-dimensional semiconductors. Nature Communications, 2015, 6, 7749.	12.8	213
8	Entropy-driven structural transition and kinetic trapping in formamidinium lead iodide perovskite. Science Advances, 2016, 2, e1601650.	10.3	203
9	Magnetism in All-Carbon Nanostructures with Negative Gaussian Curvature. Physical Review Letters, 2003, 91, 237204.	7.8	200
10	Nature of the band gap and origin of the electro-/photo-activity of Co3O4. Journal of Materials Chemistry C, 2013, 1, 4628.	5.5	176
11	Structure and Formation Mechanism of Black TiO ₂ Nanoparticles. ACS Nano, 2015, 9, 10482-10488.	14.6	170
12	Highly sensitive phototransistors based on two-dimensional GaTe nanosheets with direct bandgap. Nano Research, 2014, 7, 694-703.	10.4	140
13	Diamond fragments as building blocks of functional nanostructures. Physical Review B, 2004, 70, .	3.2	137
14	Origin of long lifetime of band-edge charge carriers in organic–inorganic lead iodide perovskites. Proceedings of the National Academy of Sciences of the United States of America, 2017, 114, 7519-7524.	7.1	137
15	Low Energy Implantation into Transition-Metal Dichalcogenide Monolayers to Form Janus Structures. ACS Nano, 2020, 14, 3896-3906.	14.6	136
16	Spectroscopic characterization of Stone-Wales defects in nanotubes. Physical Review B, 2004, 69, .	3.2	134
17	Surface-Induced Orientation Control of CuPc Molecules for the Epitaxial Growth of Highly Ordered Organic Crystals on Graphene. Journal of the American Chemical Society, 2013, 135, 3680-3687.	13.7	125
18	Tailoring Vacancies Far Beyond Intrinsic Levels Changes the Carrier Type and Optical Response in Monolayer MoSe _{2â^‹i>x} Crystals. Nano Letters, 2016, 16, 5213-5220.	9.1	121

#	Article	IF	CITATIONS
19	Persistent Step-Flow Growth of Strained Films on Vicinal Substrates. Physical Review Letters, 2005, 95, 095501.	7.8	119
20	Binding and Diffusion of Lithium in Graphite: Quantum Monte Carlo Benchmarks and Validation of van der Waals Density Functional Methods. Journal of Chemical Theory and Computation, 2014, 10, 5318-5323.	5.3	117
21	Hybrid density functional theory meets quasiparticle calculations: A consistent electronic structure approach. Physical Review B, 2013, 88, .	3.2	115
22	Van der Waals Epitaxial Growth of Two-Dimensional Single-Crystalline GaSe Domains on Graphene. ACS Nano, 2015, 9, 8078-8088.	14.6	103
23	Tunable quasiparticle band gap in few-layer GaSe/graphene van der Waals heterostructures. Physical Review B, 2017, 96, .	3.2	99
24	First-Principles Prediction of Thermodynamically Stable Two-Dimensional Electrides. Journal of the American Chemical Society, 2016, 138, 15336-15344.	13.7	91
25	Alloy Engineering of Defect Properties in Semiconductors: Suppression of Deep Levels in Transition-Metal Dichalcogenides. Physical Review Letters, 2015, 115, 126806.	7.8	81
26	Zipper Mechanism of Nanotube Fusion: Theory and Experiment. Physical Review Letters, 2004, 92, 075504.	7.8	78
27	Strain-engineered optoelectronic properties of 2D transition metal dichalcogenide lateral heterostructures. 2D Materials, 2017, 4, 021016.	4.4	72
28	Spatially resolved one-dimensional boundary states in graphene–hexagonal boron nitride planar heterostructures. Nature Communications, 2014, 5, 5403.	12.8	71
29	Solid-phase hetero epitaxial growth of α-phase formamidinium perovskite. Nature Communications, 2020, 11, 5514.	12.8	71
30	Microscopic mechanism of fullerene fusion. Physical Review B, 2004, 70, .	3.2	62
31	Model for Self-Assembly of Carbon Nanotubes from Acetylene Based on Real-Time Studies of Vertically Aligned Growth Kinetics. Journal of Physical Chemistry C, 2009, 113, 15484-15491.	3.1	59
32	Highly stable two-dimensional silicon phosphides: Different stoichiometries and exotic electronic properties. Physical Review B, 2015, 91, .	3.2	58
33	First-Principles Prediction of New Electrides with Nontrivial Band Topology Based on One-Dimensional Building Blocks. Physical Review Letters, 2018, 120, 026401.	7.8	58
34	Energetics and packing of fullerenes in nanotube peapods. Physical Review B, 2005, 71, .	3.2	48
35	Electronic Properties of Bilayer Graphene Strongly Coupled to Interlayer Stacking and an External Electric Field. Physical Review Letters, 2015, 115, 015502.	7.8	47
36	Valence band inversion and spin-orbit effects in the electronic structure of monolayer GaSe. Physical Review B, 2018, 98, .	3.2	47

#	Article	IF	CITATIONS
37	Strain tolerance of two-dimensional crystal growth on curved surfaces. Science Advances, 2019, 5, eaav4028.	10.3	46
38	Revealing the Preferred Interlayer Orientations and Stackings of Twoâ€Dimensional Bilayer Gallium Selenide Crystals. Angewandte Chemie - International Edition, 2015, 54, 2712-2717.	13.8	45
39	Observation of two distinct negative trions in tungsten disulfide monolayers. Physical Review B, 2015, 92, .	3.2	44
40	Formation of Ideal Rashba States on Layered Semiconductor Surfaces Steered by Strain Engineering. Nano Letters, 2016, 16, 404-409.	9.1	44
41	Phonon transport at the interfaces of vertically stacked graphene and hexagonal boron nitride heterostructures. Nanoscale, 2016, 8, 4037-4046.	5.6	38
42	Onset of nanotube decay under extreme thermal and electronic excitations. Physica B: Condensed Matter, 2002, 323, 78-85.	2.7	37
43	Benchmarking van der Waals density functionals with experimental data: potential-energy curves for H ₂ molecules on Cu(111), (100) and (110) surfaces. Journal of Physics Condensed Matter, 2012, 24, 424213.	1.8	35
44	Exceptional Optoelectronic Properties of Hydrogenated Bilayer Silicene. Physical Review X, 2014, 4, .	8.9	35
45	Doping transition-metal atoms in graphene for atomic-scale tailoring of electronic, magnetic, and quantum topological properties. Carbon, 2021, 173, 205-214.	10.3	35
46	Energetics and kinetics of Ti clustering on neutral and charged C60 surfaces. Journal of Chemical Physics, 2008, 129, 134707.	3.0	34
47	Nonequilibrium Synthesis of TiO ₂ Nanoparticle "Building Blocks―for Crystal Growth by Sequential Attachment in Pulsed Laser Deposition. Nano Letters, 2017, 17, 4624-4633.	9.1	33
48	Dynamics of Step Bunching in Heteroepitaxial Growth on Vicinal Substrates. Physical Review Letters, 2007, 99, 055503.	7.8	31
49	Nitrogen Doping Enables Covalent-Like π–π Bonding between Graphenes. Nano Letters, 2015, 15, 5482-5491.	9.1	31
50	Growth of Metal Phthalocyanine on Deactivated Semiconducting Surfaces Steered by Selective Orbital Coupling. Physical Review Letters, 2015, 115, 096101.	7.8	30
51	Influence of defects and doping on phonon transport properties of monolayer MoSe ₂ . 2D Materials, 2018, 5, 031008.	4.4	30
52	GPU acceleration of all-electron electronic structure theory using localized numeric atom-centered basis functions. Computer Physics Communications, 2020, 254, 107314.	7.5	30
53	Effect of Metal Doping and Vacancies on the Thermal Conductivity of Monolayer Molybdenum Diselenide. ACS Applied Materials & Interfaces, 2018, 10, 4921-4928.	8.0	29
54	Metastable Li _{1+δ} Mn ₂ O ₄ (0 â‰ቑ´â‰¤1) Spinel Phases Revealed by in Operando Neutron Diffraction and First-Principles Calculations. Chemistry of Materials, 2019, 31, 124-134.	6.7	28

#	Article	IF	CITATIONS
55	Polygonization and anomalous graphene interlayer spacing of multi-walled carbon nanofibers. Physical Review B, 2007, 75, .	3.2	26
56	Finite-Temperature Hydrogen Adsorption and Desorption Thermodynamics Driven by Soft Vibration Modes. Physical Review Letters, 2013, 111, 066102.	7.8	25
57	Doping of Cr in Graphene Using Electron Beam Manipulation for Functional Defect Engineering. ACS Applied Nano Materials, 2020, 3, 10855-10863.	5.0	24
58	Can photo excitations heal defects in carbon nanotubes?. Chemical Physics Letters, 2004, 392, 209-213.	2.6	23
59	Electron transfer and localization in endohedral metallofullerenes: <i>Ab initio</i> density functional theory calculations. Physical Review B, 2008, 78, .	3.2	23
60	Interaction between hydrogen molecules and metallofullerenes. Journal of Chemical Physics, 2009, 131, 064707.	3.0	22
61	The Role of Interfacial Electronic Properties on Phonon Transport in Two-Dimensional MoS ₂ on Metal Substrates. ACS Applied Materials & Interfaces, 2016, 8, 33299-33306.	8.0	21
62	Understanding the Charge Transfer at the Interface of Electron Donors and Acceptors: TTF–TCNQ as an Example. ACS Applied Materials & Interfaces, 2017, 9, 27266-27272.	8.0	21
63	Strain-Induced Growth of Twisted Bilayers during the Coalescence of Monolayer MoS ₂ Crystals. ACS Nano, 2021, 15, 4504-4517.	14.6	19
64	GPU-acceleration of the ELPA2 distributed eigensolver for dense symmetric and hermitian eigenproblems. Computer Physics Communications, 2021, 262, 107808.	7.5	19
65	Understanding the Metal-Directed Growth of Single-Crystal M-TCNQF ₄ Organic Nanowires with Time-Resolved, in Situ X-ray Diffraction and First-Principles Theoretical Studies. Journal of the American Chemical Society, 2012, 134, 14353-14361.	13.7	17
66	Interplay between intercalated oxygen superstructures and monolayer <mml:math xmlns:mml="http://www.w3.org/1998/Math/MathML"><mml:mi>h</mml:mi>-BN on Cu(100). Physical Review B, 2016, 94, .</mml:math 	3.2	16
67	Surface Magnetism of Cobalt Nanoislands Controlled by Atomic Hydrogen. Nano Letters, 2017, 17, 292-298.	9.1	15
68	Selective Antisite Defect Formation in WS ₂ Monolayers via Reactive Growth on Dilute Wâ€Au Alloy Substrates. Advanced Materials, 2022, 34, e2106674.	21.0	14
69	Antiferromagnetic Order and Linear Magnetoresistance in Fe-Substituted Shandite Co ₃ In ₂ S ₂ . Chemistry of Materials, 2021, 33, 9741-9749.	6.7	14
70	Stabilized Synthesis of 2D Verbeekite: Monoclinic PdSe ₂ Crystals with High Mobility and In-Plane Optical and Electrical Anisotropy. ACS Nano, 2022, 16, 13900-13910.	14.6	14
71	First-principles studies of hydrogen interaction with ultrathin Mg and Mg-based alloy films. Physical Review B, 2011, 83, .	3.2	13
72	Cobalt-based magnetic Weyl semimetals with high-thermodynamic stabilities. Npj Computational Materials, 2021, 7, .	8.7	13

#	Article	IF	CITATIONS
73	Revealing the Chemical Bonding in Adatom Arrays via Machine Learning of Hyperspectral Scanning Tunneling Spectroscopy Data. ACS Nano, 2021, 15, 11806-11816.	14.6	13
74	Equilibrium structure of ferrofluid aggregates. Journal of Physics Condensed Matter, 2010, 22, 455105.	1.8	12
75	Weak competing interactions control assembly of strongly bonded TCNQ ionic acceptor molecules on silver surfaces. Physical Review B, 2014, 90, .	3.2	11
76	Phonon transport properties of two-dimensional electride Ca2N—A first-principles study. Applied Physics Letters, 2018, 113, .	3.3	11
77	Quantum Phase Engineering of Two-Dimensional Post-Transition Metals by Substrates: Toward a Room-Temperature Quantum Anomalous Hall Insulator. Nano Letters, 2020, 20, 7186-7192.	9.1	9
78	Enhanced dipole moments in photo-excited TTF–TCNQ dimers. New Journal of Physics, 2011, 13, 073039.	2.9	8
79	Understanding Heterogeneities in Quantum Materials. Advanced Materials, 2023, 35, e2106909.	21.0	8
80	Boundary effects on dynamic behavior of Josephson-junction arrays. Physical Review B, 2000, 62, 5357-5360.	3.2	7
81	How the shape of catalyst nanoparticles determines their crystallographic orientation during carbon nanofiber growth. Carbon, 2013, 60, 41-45.	10.3	7
82	Crystal structures and rotational dynamics of a two-dimensional metal halide perovskite (OA)2PbI4. Journal of Chemical Physics, 2020, 152, 014703.	3.0	7
83	Understanding Substrate-Guided Assembly in van der Waals Epitaxy by <i>in Situ</i> Laser Crystallization within a Transmission Electron Microscope. ACS Nano, 2021, 15, 8638-8652.	14.6	7
84	Temporally decoherent and spatially coherent vibrations in metal halide perovskites. Physical Review B, 2020, 102, .	3.2	7
85	Lattice effects on the current-voltage characteristics of superconducting arrays. Physical Review B, 2000, 61, 3263-3266.	3.2	6
86	Recent advances in computational materials design: methods, applications, algorithms, and informatics. Journal of Materials Science, 2022, 57, 10471-10474.	3.7	6
87	Revealing the Preferred Interlayer Orientations and Stackings of Twoâ€Đimensional Bilayer Gallium Selenide Crystals. Angewandte Chemie, 2015, 127, 2750-2755.	2.0	5
88	Assessing the Predictive Power of Density Functional Theory in Finite-Temperature Hydrogen Adsorption/Desorption Thermodynamics. Journal of Physical Chemistry C, 2018, 122, 26189-26195.	3.1	5
89	Targeted medication delivery using magnetic nanostructures. Journal of Physics Condensed Matter, 2007, 19, 086210.	1.8	4
90	A hybrid optimization algorithm to explore atomic configurations of TiO2 nanoparticles. Computational Materials Science, 2018, 141, 1-9.	3.0	4

#	Article	IF	CITATIONS
91	Laser Interactions for the Synthesis and In Situ Diagnostics of Nanomaterials. Springer Series in Materials Science, 2014, , 143-173.	0.6	4
92	Floquet band engineering and topological phase transitions in 1T' transition metal dichalcogenides. 2D Materials, 2022, 9, 025005.	4.4	4
93	Self-regulated growth of candidate topological superconducting parkerite by molecular beam epitaxy. APL Materials, 2021, 9, 101110.	5.1	3
94	Performance of biologically inspired algorithms tuned on TiO2 nanoparticle benchmark system. Computational Materials Science, 2019, 165, 63-73.	3.0	2
95	Topography inversion in scanning tunneling microscopy of single-atom-thick materials from penetrating substrate states. Scientific Reports, 2022, 12, 7321.	3.3	2
96	Laser Synthesis, Processing, and Spectroscopy of Atomically-Thin Two Dimensional Materials. Springer Series in Materials Science, 2018, , 1-37.	0.6	1
97	Emerging edge states on the surface of the epitaxial semimetal CuMnAs thin film. Applied Physics Letters, 2020, 116, 061603.	3.3	1
98	Phase Transformations and Surface/Interface Properties in Functional Perovskites with Aberration-Corrected STEM/EELS. Microscopy and Microanalysis, 2015, 21, 2429-2430.	0.4	0
99	A first-principles study of phonon transport properties of monolayer MoSe <inf>2</inf> . , 2017, , .		0